Langmuir

Article

pubs.acs.org/Langmuir

Phototriggered Functionalization of Hierarchically Structured Polymer Brushes

Andres de los Santos Pereira,[†] Nina Yu. Kostina,[†] Michael Bruns,[‡] Cesar Rodriguez-Emmenegger,*[,†] and Christopher Barner-Kowollik*[,∥,§]

[†]Institute of Macromolecular Chemistry, Academy of Sciences of the Czech Republic, v.v.i., Heyrovsky sq. 2, 162 06 Prague, Czech Republic

[‡]Institut für Angewandte Materialien (IAM), Karlsruhe Nano Micro Facility (KNMF), Karlsruhe Institute of Technology (KIT), Hermann-von-Helmholtz-Platz 1, 76344 Eggenstein-Leopoldshafen, Germany

[∥]Preparative Macromolecular Chemistry, Institut für Technische Chemie und Polymerchemie, Karlsruhe Institute of Technology (KIT), Engesserstr. 18, 76131 Karlsruhe, Germany

[§]Institut für Biologische Grenzflächen, Karlsruhe Institute of Technology (KIT), Hermann-von-Helmholtz-Platz 1, 76344 Eggenstein-Leopoldshafen, Germany

Supporting Information

ABSTRACT: The precise design of bioactive surfaces, essential for the advancement of many biomedical applications, depends on achieving control of the surface architecture as well as on the ability to attach bioreceptors to antifouling surfaces. Herein, we report a facile avenue toward hierarchically structured antifouling polymer brushes of oligo(ethylene glycol) methacrylates via surface-initiated atom transfer radical polymerization (SI-ATRP) presenting photoactive tetrazole moieties, which permitted their functionalization via nitrile imine-mediated tetrazole-ene cycloaddition (NITEC). A maleimide-functional ATRP initiator was photoclicked to the side chains of a brush enabling a subsequent polymerization of carboxybetaine acrylamide to generate a micropatterned *graft-on-graft* polymer architecture as evidenced by X-ray photoelectron spectroscopy (XPS) and time-of-flight secondary ion mass spectrometry (ToF-SIMS). Furthermore, the spatially resolved biofunctionalization of the tetrazole-presenting brushes was accessed by the photoligation of biotin-maleimide and subsequent binding of streptavidin. The functionalized brushes bearing streptavidin were able to resist the fouling from blood plasma (90% reduction with respect to bare gold). Moreover, they were employed to demonstrate a model biosensor by immobilization of a biotinylated antibody and subsequent capture of an antigen as monitored in real time by surface plasmon resonance.

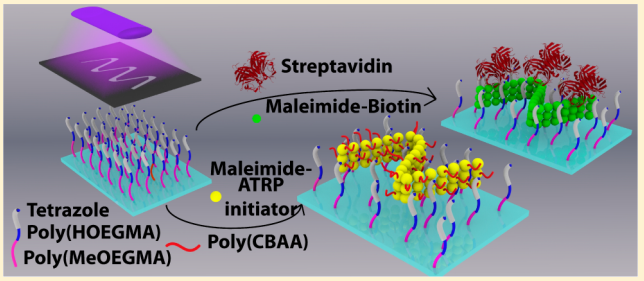

INTRODUCTION

The control of the interactions of biological molecules at the interface between artificial surfaces and biological systems is critical for the success of devices that operate in direct contact with biological fluids and environments.[1,2] These include biosensors, tissue engineering scaffolds, and bioimplants.[3] For this purpose, precisely engineered bioactive surfaces can be achieved by the controlled grafting of well-defined polymer layers.[4] In particular, polymer brushes show great promise and have begun to be applied in research.[5−10] Arguably, a carefully designed macromolecular architecture plays a fundamental role in these systems, determining the performance of the surfaces under study and expanding the synthetic tool box available for the polymer chemist.[4,9,11] The architecture of the polymer brushes has been shown to critically determine the properties, including the resistance to fouling, immobilization capacity of bioreceptors, and stimuli-responsive behavior.[11−13] Of the myriad of synthetic techniques that have been developed in recent years, controlled radical polymerization and modular ligations (often adhering to the click chemistry criteria) are among the most valuable tools available for this purpose.[14] Surface-initiated atom transfer radical polymerization (SI-ATRP) provides a versatile route to build polymer layers on a surface via a "grafting from" approach with a vast array of available monomers to provide the desired properties and functionalities.[4,9,10]

Moreover, the postpolymerization modification of the polymer architectures obtained via "grafting-from" processes further expands the accessible functionalities and allows for the binding of bioreceptors onto the surface.[15−18] The tailoring of the surface properties and its interactions with biological media requires the immobilization of bioactive motifs on the surface,

Received: March 28, 2015
Revised: May 9, 2015

DOI: 10.1021/acs.langmuir.5b01114
Langmuir XXXX, XXX, XXX−XXX

such as biorecognition elements in the case of biosensors[19] or cell attachment cues for scaffolds for tissue engineering.[20,21] In this context, the ability to achieve spatial control of the reaction is a requirement for several applications. In the design of high-throughput biosensors and DNA/protein arrays, the location on the surface of the biomolecules must be precisely controlled.

Previously, we reported the use of a catalyst-free ligation reaction to achieve the rapid biofunctionalization of polymer brushes under mild conditions without the need for a catalyst, taking advantage of the polymer end groups.[22] Nevertheless, the ability to address only selected sites or areas for the functionalization can be accessed by employing phototriggered ligation reactions.[23] Photoactivated reactions including thiol−ene coupling,[24,25] strain-promoted alkyne−azide cycloaddition,[26] those employing a photocaged diene in a Diels−Alder ligation,[23,27] or nitrile imine-mediated tetrazole-ene cycloadditions[5,28] (NITEC) as well as the reaction of photogenerated thioaldehydes with nucleophiles or dienes[29] have been used on surfaces to achieve their functionalization in a spatially selective manner. NITEC—the reaction between a nitrile imine dipole and a dipolarophile such as an alkene or alkyne—in particular presents several advantages, such as high selectivity, bioorthogonality, and sensitivity to relatively long wavelengths of UV light.[3,5,30] The irradiation of a diaryl tetrazole with UV-light generates the highly reactive nitrile imine coupled with the release of N_2, while the absorption peak of the transition can be conveniently tuned by the selection of the substituents.[31] The application of NITEC for the functionalization of a poly(dopamine)-coated surface allowed to spatially confine the growth of antifouling polymer brushes, capable of preventing cell adhesion, effectively achieving the high fidelity patterning of cells.[5]

Herein, we present the application of the phototriggered NITEC reaction for the spatially resolved (bio)-functionalization of hierarchically structured polymer brushes, demonstrated by the immobilization of biotin and the subsequent capture of streptavidin, which is subsequently exploited to demonstrate a model label-free biosensing platform. Moreover, the patterning of an ATRP-initiator moiety on the side chains of the brushes is carried out. Thus, the control of the macromolecular architecture is simultaneously achieved, taking advantage of the successive SI-ATRP of different monomers to generate graft-on-graft structures. Thus, the chemical route reported provides access to antifouling polymer brushes of controlled macromolecular architecture that can be biofunctionalized in a spatially resolved manner.

EXPERIMENTAL SECTION

Materials. Oligo(ethylene glycol) methyl ether methacrylate (M_n = 300 g·mol^{-1}, MeOEGMA), oligo(ethylene glycol) methacrylate (M_n = 500 g·mol^{-1}, HOEGMA), $CuBr_2$ (99%), CuBr (99.99%), 2,2′-bipyridyl (99%), 1,4,8,11-tetramethyl-1,4,8,11-tetraazacyclotetradecane (Me_4Cyclam, 98%), triethylamine (TEA, 99%) NaN_3 (99%), maleimide-biotin (*N*-biotinoyl-*N*′-(6-maleimidohexanoyl) hydrazide, ≥95%), and human serum were purchased from Sigma−Aldrich, Czech Republic. Streptavidin, biotin-conjugated rabbit IgG, biotin-conjugated goat IgG anti(mouse IgG), and mouse IgG were purchased from Thermo Fisher Scientific, Czech Republic. Human blood plasma (mix from 5 donors) was provided by the Institute of Hematology and Blood Transfusion, Czech Republic. ω-Mercaptoundecyl bromoisobutyrate and (3-acryloylaminopropyl)-(2-carboxyethyl)-dimethylammonium (CBAA) were synthesized according to procedures published earlier.[32,33] The tetrazole acid chloride (4-(2-(4-methoxyphenyl)-2H-tetrazol-5-yl)benzoic acid chloride) and the maleimide-conjugated ATRP initiator (2-bromo-2-methyl propionic acid 2-(3,5-dioxo-10-oxa-4-aza-tricyclo[5.2.1.0^{2,6}]dec-8-en-4-yl) ethyl ester) were synthesized according to our previously published methods.[5]

Self-Assembled Monolayer (SAM) of the ATRP Initiator. The substrates used for all experiments except surface plasmon resonance (SPR) were silicon wafer chips (1 cm × 1 cm) coated with an intermediate titanium layer for adhesion (2 nm) and a thin layer of gold on the surface (about 150 nm). For surface plasmon resonance, the substrates used were microscope glass slides coated with a titanium adhesion layer and 50 nm of gold. The chips were rinsed with ethanol followed by deionized water twice, blow dried with nitrogen, and air plasma cleaned for 20 min. Subsequently, the wafers were immediately placed in a 1 mM solution of ω-mercaptoundecyl bromoisobutyrate in absolute ethanol and kept overnight at room temperature to form the initiator SAM. After rinsing with ethanol and water, the samples were blow dried with nitrogen.

ATRP of the Bottom Block of the Polymer Brush. Three round-bottom flasks containing: (1) methanol, (2) a solution of MeOEGMA (M_n = 300 g·mol^{-1}, 5.7 g, 19 mmol) in 5 mL of water, and (3) 2,2′-bipyridyl (155 mg, 991 μmol), $CuBr_2$ (16.8 mg, 75 μmol), and $CuBr_2$ (53.8 mg, 375 μmol) were deoxygenated separately by bubbling with Ar for 1 h. Methanol (5 mL) was transferred under Ar-protection from flask 1 to flask 3, which was stirred until dissolution. Subsequently, the monomer solution was transferred under Ar-protection from flask 2 to flask 3 and thoroughly mixed. The polymerization mixture was transferred to Ar-filled reactors containing the substrates coated with initiator SAM. The reaction was allowed to proceed at 30 °C for 15 min and then stopped by removing the chips from the solution and rinsing them with ethanol and water, and blow drying with nitrogen.

Diblock Architecture via ATRP. The top block of poyl-(HOEGMA) was grown according to the same procedure employed for the bottom poly(MeOEGMA) block. The monomer employed was HOEGMA (M_n = 500 g·mol^{-1}, 9.5 g, 19 mmol) for the same quantities of all other reagents. The substrates employed were already coated with the poly(MeOEGMA) brushes which served as macro-initiators. The reaction proceeded for 30 min at 30 °C.

Deactivation of the Br End Groups by Nucleophilic Substitution. NaN_3 (51 mg, 785 μmol) was dissolved in 15 mL of anhydrous dimethylformamide (DMF). The solution was deoxygenated by bubbling of Ar and transferred to Ar-filled reactors containing the poly(MeOEGMA-*b*-HOEGMA)-coated substrates. The reaction proceeded at 50 °C for 3 h. Finally, the wafers were rinsed with DMF, ethanol, and deionized water, and blow dried with nitrogen.

Decoration of the Surface with Tetrazole Acid Chloride. The tetrazole acid chloride was reacted with the hydroxy groups in the side chains of the poly(HOEGMA) block of the brushes.[5,34] The substrates were placed in 30 mL of a 0.12 M solution of TEA (364 mg, 502 μL) in tetrahydrofuran (THF) at ambient temperature. Fifteen milliliters of a 0.12 M solution of tetrazole chloride (565 mg) in THF were added dropwise and the reaction was allowed to proceed under gentle shaking for 1 h. After rinsing with THF, dichloromethane (DCM), ethanol, and deionized water, the samples were blow dried with nitrogen and kept in the dark.

Phototriggered Click Reactions. The phototriggered immobilizations of both maleimide-biotin (for subsequent biofunctionalization) and maleimide-ATRP-initiator (for formation of graft-on-graft structures) were carried out employing the same procedure. The tetrazole-functionalized polymer brushes samples were placed vertically in individual headspace vials. In the case of the samples on which patterning was conducted for ToF-SIMS imaging, the sample was placed in a sample holder with a shadow mask on top of the surface.[28] The vials were filled with sufficient volume to cover the sample of a solution of either maleimide-biotin (1 mg·mL^{-1} in dry DMF) or maleimide-ATRP-initiator (1 mg·mL^{-1} in dry DCM), crimped airtight, and purged with nitrogen for 5 min in the dark to remove atmospheric oxygen and avoid undesired photooxidation reactions. The samples to be irradiated were placed in a custom-made

DOI: 10.1021/acs.langmuir.5b01114
Langmuir XXXX, XXX, XXX−XXX

Scheme 1. Chemical Route Employed for the Generation of the Tetrazole-Functional Hierarchically Structured Polymer Brushes and Their Subsequent Functionalization

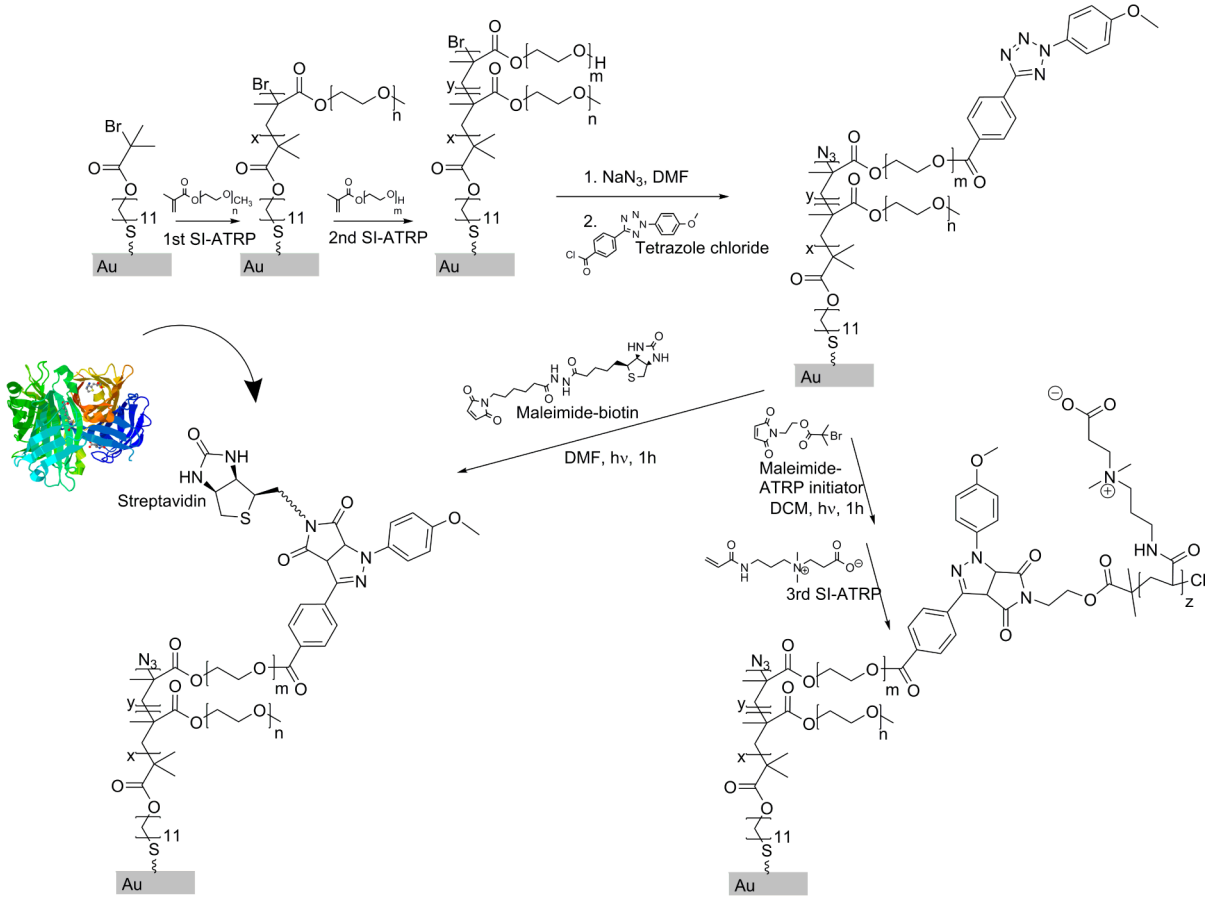

photoreactor suspended from a metallic disk (diameter 4−5 cm) slowly revolving around a compact low-pressure lamp (Arimed B6, Cosmedico GmbH, Germany) emitting at λ = 320 nm (±30 nm, 36 W, the emission spectrum of the UV-lamp employed is shown elsewhere[5]). After 1 h of irradiation, the vials were opened, and the samples removed and rinsed copiously with the solvent used for the corresponding reaction (either DMF or DCM), followed by ethanol and water, and dried by blow drying with nitrogen.

Biofunctionalization with Streptavidin. The substrates coated with maleimide-biotin-functionalized polymer brushes were placed in individual vials and covered with a 0.5 mg·mL^{-1} solution of streptavidin in phosphate buffered saline (PBS, pH 7.4). After 3 h of contact the samples were rinsed with abundant PBS, followed by water, and dried by gentle blowing of nitrogen.

Preparation of a Model Biosensing Platform. SPR chips coated with biotin-presenting polymer brushes were biofunctionalized in situ in the SPR setup. After establishing a baseline in PBS, a solution of streptavidin (100 μg·mL^{-1} in PBS) was injected over the surface and replaced with PBS after 30 min. Subsequently, on two independent channels solutions of biotinylated nonspecific rabbit IgG or biotinylated goat polyclonal antibody against mouse IgG (50 μg·mL^{-1} in PBS) were flowed for 10 min and replaced with PBS. The capture capacity and specificity of the sensing surfaces obtained were then tested by simultaneously injecting in both channels for 10 min a 50 μg·mL^{-1} solution of mouse IgG in PBS.

Poly(carboxybetaine acrylamide) Graft-on-Graft. The polymerization of CBAA was carried out according to our previously published procedure.[33] PBS (10 mL) was degassed by three cycles of freeze−pump−thaw and transferred under inert atmosphere to a degassed Schlenk flask containing CuBr (19.1 mg, 133 μmol), $CuBr_2$ (5.9 mg, 26.5 μmol), and Me_4Cyclam (40.9 mg, 160 μmol). After dissolution, the catalyst mixture was transferred to a Schlenk flask containing CBAA (1.5 g, 6.7 mmol) and stirred. The polymerization solution was transferred to Ar-filled reactors containing the substrates coated with the polymer brushes functionalized with maleimide-ATRP-initiator and left to react for 2 h at 30 °C. The reactors were subsequently opened and the substrates removed, rinsed with water, ethanol, and finally water, and blow dried with nitrogen

Ellipsometry. The dry thickness of the layers after each relevant modification step was measured by ellipsometry using a Variable Angle Spectroscopic Imaging Auto-Nulling Ellipsometer EP3-SE (Nanofilm Technologies GmbH, Germany) with a laser at a wavelength λ = 532 nm at angles of incidence AOI = 60, 65, and 70° in air at room temperature. The data were fitted using multilayer models with the EP4Model analysis software.

X-ray Photoelectron Spectroscopy (XPS). XPS measurements were carried out with a K-Alpha XPS spectrometer (Thermo Fisher Scientific, East Grinstead, UK). The samples were analyzed using a microfocused, monochromated Al Kα X-ray source (400 μm spot size). The kinetic energy of the electrons was measured using a 180° hemispherical energy analyzer operated in the constant analyzer energy mode (CAE) at 50 eV pass energy for elemental spectra. Data acquisition and processing using the Thermo Avantage software is described elsewhere.[35]

The spectra were fitted with one or more Voigt profiles (binding energy uncertainty: ± 0.2 eV). The analyzer transmission function, Scofield sensitivity factors,[36] and effective attenuation lengths (EALs) for photoelectrons were applied for quantification. EALs were calculated using the standard TPP-2M formalism.[37] All spectra were referenced to the C 1s peak of hydrocarbons at 285.0 eV binding energy controlled by means of the well-known photoelectron peaks of metallic Cu, Ag, and Au.

Time-of-Flight Secondary Ion Mass Spectrometry (ToF-SIMS). Imaging by ToF-SIMS was performed on a TOF.SIMS-V

DOI: 10.1021/acs.langmuir.5b01114
Langmuir XXXX, XXX, XXX−XXX

instrument (ION-TOF GmbH, Münster, Germany) equipped with a Bi cluster liquid metal primary ion source and a nonlinear time-of-flight analyzer. The Bi source was operated in the "bunched" mode, providing 0.7 ns Bi^+ ion pulses at 25 keV energy and a lateral resolution of ~4 μm. The short pulse length allowed for high mass resolution to analyze the complex mass spectra of the immobilized organic layers. Images larger than the maximum deflection range of the primary ion gun of 500 × 500 μm^2 were obtained using the manipulator stage scan mode. Negative polarity spectra were calibrated on the C^-, C^{2-}, C^{3-}, and Br^- peaks. Primary ion doses were kept below 10^{11} ions·cm^{-2} (static SIMS limit).

Surface Plasmon Resonance (SPR). The immobilization of streptavidin and biotin-conjugated antibodies on biotin-functionalized polymer brushes was followed by SPR using an instrument based on the Kretschmann configuration and spectral interrogation, monitoring the resonance wavelength λ_{res}. The temperature was set at 25 °C, and all solutions were flowed through the flow cell at 25 μL·min^{-1}. After a stable baseline was achieved in PBS (pH 7.4), the solutions were injected in the flow cell for a specified time and subsequently replaced by PBS. The fouling was measured from undiluted human blood plasma after 15 min of contact. The sensor response is recorded as the difference in resonance wavelength $\Delta\lambda_{res}$ before and after contact with the solutions and is proportional to the mass deposited on the surface.[16]

RESULTS AND DISCUSSION

Preparation of Polymer Brushes Bearing Photofunctonalizable Side Groups. Antifouling polymer brushes consisting of two blocks were grown as depicted in Scheme 1.[16,33] A SAM of ATRP initiator was prepared on the surface of gold-coated silicon wafer substrates. Polymer brushes of oligo(ethylene glycol) methyl ether methacrylate were grafted from the surface, and subsequently a second block of hydroxy-functional oligo(ethylene glycol) methacrylate was grown. The use of gold as a model surface was chosen due to the importance of this material in biosensor transducers[38] and the simplicity with which polymer brushes can be grafted from and characterized on a SAM of thiol-containing initiator molecules.[16] Nevertheless, the approach does not restrict the general applicability of the procedure, since such functional polymer brushes can be grown on virtually any substrate through the use of an appropriate linker specific for the material of interest or a substrate-independent adlayer such as poly(dopamine).[34,39−41]

The success of each step in the modification of the surfaces to achieve the desired structures was confirmed by monitoring the dry layer thickness by ellipsometry and the chemical composition by XPS. The formation of the initiator SAM can be observed in the XPS spectrum of the C 1s region (Figure 1A) showing the predominance of C−C and C−H bonds of the alkane backbone at 285.0 eV as well as the O−C═O peak of the initiator ester moiety. The presence of Br forming C−Br bonds, entailed in the initiator group, is also detected on the surface (Figure 1B). The contributions arising from Br^- ions are caused by decomposition due to the irradiation with X-rays during analysis. The C 1s spectra for both types of polymer brushes, poly(MeOEGMA) and poly(MeOEGMA-*b*-HOEGMA), share a predominance of carbon in the C−O bonds seen at 286.4 eV (Figure 1A). The methacrylate ester group appears close to 289.9 eV. It is interesting to note how the ratio of the C−O to O−C═O peak increases when going from pure poly(MeOEGMA) to the diblock polymer brush. This can be explained by the higher number of ethylene glycol units in the longer oligo(ethylene glycol) side chains of HOEGMA. A thickness of 15 nm was obtained for the first polymer block,

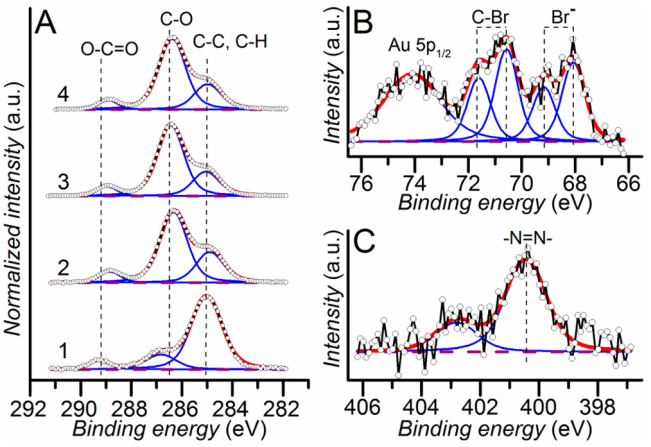

Figure 1. (A) High-resolution XPS spectrum of the C 1s region of the surface modification steps: (1) initiator SAM, (2) poly(MeOEGMA), (3) poly(MeOEGMA-*b*-HOEGMA), and (4) tetrazole-functionalized polymer brush. (B) High-resolution XPS spectrum of the Br 3d region of the initiator SAM. (C) High-resolution XPS spectrum of the N 1s region of the tetrazole-functional polymer brush.

while the growth of a second block caused an increase in thickness of 21 nm to reach a total of 35 nm (Table 1).

Table 1. Dry Layer Thickness of the Polymer Brushes

surface	thickness/nm
initiator SAM	1
poly(MeOEGMA)	15
poly(MeOEGMA-*b*-HOEGMA)	36

The well-controlled nature of the SI-ATRP process of the methacrylate monomers[16] makes it possible to reinitiate the polymerization centers and obtain a diblock bottle brush architecture in which the side groups of the polymer chains present hydroxy functionalities only along a desired top region of the polymer chain. These functional groups are subsequently addressed during the arylation with the photoactive tetrazole. In comparison with the chain end approach for the modification of polymer brushes, this route has the advantage of enabling the tuning of the extent of the functional group desired modification by adjusting the length of the two blocks, which can be achieved simply by varying the polymerization times of each step.[40] The thicknesses selected for the two blocks of the polymer brushes are consistent with what has been observed in our previous work to yield good results for resistance to protein fouling and functionalization capacity.[40,42] In order to prevent the growth from the polymer end groups in subsequent ATRP steps, the Br end groups were removed by a nucleophilic substitution with NaN_3.

To address the requirements for more complex macromolecular architectures and spatially resolved biofunctionalization of the polymer brushes, we introduced tetrazole groups onto their side chains after polymerization. These groups can be subsequently addressed by the photoactivated NITEC reaction to ligate the desired molecules to the surface. Immobilization of the tetrazole moiety on the top block of the polymer layer was achieved by the arylation of the hydroxy groups of the polymer side chains with the acyl chloride form of the tetrazole in dry THF for 1 h. The thickness of the layer did not appreciably increase after the reaction. However, the high-resolution XPS spectrum of the N 1s region clearly shows the

DOI: 10.1021/acs.langmuir.5b01114
Langmuir XXXX, XXX, XXX−XXX

appearance of a signal at 400.5 and 402.8 eV, which corresponds to the expected tetrazole species (−N═N−) and probably positively charged nitrogen, respectively (Figure 1C).[28] The contributions observed in the XPS spectrum of the C 1s region of the tetrazole-functionalized polymer brushes indicate a predominance of the features corresponding to the polymer (Figure 1A).

Encoding Biofunctionality by Photopatterning of Biotion and Capture of Streptavidin. The tetrazole-functional polymer brushes were employed to biofunctionalize the surface with streptavidin. This protein is an ideal choice to assess the biofunctionalization of these surfaces, as it can bind to a wide range of bioreceptors conjugated with biotin. Thus, a generic platform allowing for the further encoding of variable biofunctionalities can be achieved. Initially, the phototriggered and spatially resolved immobilization of a maleimide-functional biotin was carried out. The biotin−streptavidin couple displays one of the highest affinities of noncovalent interactions known, characterized by an extremely low dissociation constant, $K_D \approx 10^{-14}$ M, which was further exploited to decorate the surfaces with streptavidin biomolecules. To achieve the immobilization of biotin on the tetrazole-containing polymer side chains, the samples were contacted with a 1 mg·mL^{-1} maleimide−biotin solution in DMF in a crimped headspace vial, purged with nitrogen to remove atmospheric oxygen and irradiated for 1 h with a UV lamp, λ_{max} = 320 nm. The use of a tetrazole with a methoxy substituent in the *para* position of the N2 in the ring enables the photoactivation to occur under UV irradiation of relatively long wavelengths, resulting in milder ligation conditions.[5] This fact, together with the removal of oxygen from the vials, helps to minimize undesired photooxidation reactions which could degrade the thiol SAM on gold,[43] with a concomitant damage to the polymer brush. The change in the XPS spectrum's N 1s region upon irradiation with UV light in the presence of biotin is consistent with the activation of the tetrazole moiety through the loss of N_2 (Table S1 in the Supporting Information). Upon contact with a 0.5 mg·mL^{-1} streptavidin solution in phosphate buffered saline (PBS, pH 7.4) for 3 h, a large increase in the signal at 400.1 eV in the XPS spectrum of the N 1s region is observed (Figure 2B and Table S1, Supporting Information), corresponding to the N atoms in the peptide bond expected in the streptavidin. Furthermore, the relative contribution of the C−O bonds, corresponding to the ethylene glycol units of the underlying polymer brush, decreases in comparison to the C−C, C−H, and O−C═O more prevalent in the protein (Figure 2).

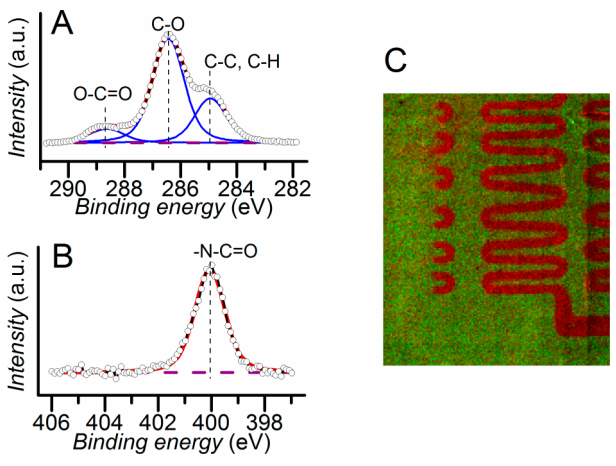

Figure 2. Functionalization with streptavidin. High-resolution XPS spectra of the C 1s (A) and N 1s (B) regions. (C) ToF-SIMS image showing an overlay of CN^- (red) stemming from protein fragments and $C_7H_4N^-$ (green) arising from the unreacted tetrazole.

To demonstrate the spatial control of the functionalization achievable by directing and restricting the irradiation with UV light, a shadow mask was employed, followed by contact with a streptavidin solution under the same conditions as described above. ToF-SIMS was subsequently employed to map the surface according to the presence of specific fragments that can be correlated to the expected chemical structures (refer to Figure 2C). The image obtained for the nitrogen-containing residue CN^- stemming from protein residues[28] clearly follows the wave-like pattern, with a sharp increase in the irradiated area, in which biotin was expected to be immobilized, indicating the presence of streptavidin with its protein structure. Furthermore, the overlay image shows the presence of the unreacted tetrazole (102.0 u, $C_7H_4N^-$) exclusively in the nonirradiated areas. It is expected that the presence of this moiety could be employed for the further functionalization of the nonirradiated areas of the surface with a different molecule. The ToF-SIMS image for the tetrazole fragment evidences the absence of unreacted groups in the area inside of the pattern after 1 h of irradiation, which might interfere in a subsequent photoligation with a different molecule (Figure S2 in the Supporting Information).

To further confirm the specificity of immobilization of streptavidin on the surface, we contacted a tetrazole-functional polymer brush with biotin in the absence of irradiation by UV-light (refer to the Supporting Information). After rinsing, the sample was contacted with a streptavidin solution and the XPS spectrum was recorded. The signal in the N 1s region corresponds to the original tetrazole, while no changes originating from a potential nonspecific adsorption of streptavidin could be detected (refer to Figure S1 in the Supporting Information), in agreement with the excellent protein resistance of the block copolymer brushes.[16,33] Importantly, the control experiment evidences that maleimide-functional biotin could only be immobilized under irradiation with UV-light. Thus, the ability to obtain a pattern of immobilized streptavidin arises both from the resistance to protein fouling provided by the polymer brushes and the requirement of a light stimulus for the functionalization reaction to proceed.

The attachment of streptavidin on the biotin-functionalized polymer brushes was also monitored by SPR. This technique is able to follow the increase in deposited mass on the surface via the changes it causes in the propagation coefficient of the surface plasmons at the interface between a metal and the solution of interest. The obtained sensogram reflects the attachment of the streptavidin (from a 100 μg·mL^{-1} solution in PBS) as a function of time on the surface presenting biotin (Figure 3A). A small decrease at the beginning of the attachment and final increase at the end of the contact period are caused by the difference in refractive indices between the PBS and the streptavidin solution in PBS. After a baseline was re-established in PBS, an immobilized amount of streptavidin of 21 ng·cm^{-2} was observed. Since no unreacted tetrazole groups were detected by ToF-SIMS in the irradiated area after 1 h of UV irradiation, longer reaction times are not expected to increase the attainable immobilized amount of biotin and streptavidin. A possible way to achieve an increase in the load

DOI: 10.1021/acs.langmuir.5b01114
Langmuir XXXX, XXX, XXX−XXX

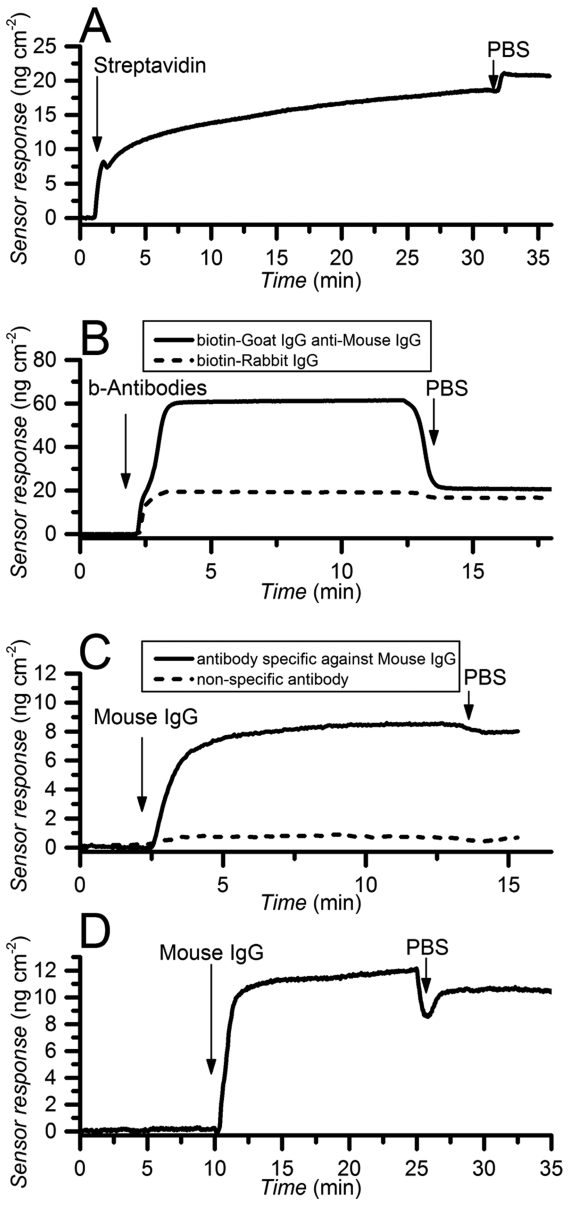

Figure 3. (A) Immobilization of streptavidin followed by SPR. (B) Capture of two different biotinylated antibodies on a streptavidin-functionalized polymer brush. (C) Specific detection of a model immunoglobulin on a channel functionalized with an antibody able to capture it. The second channel was functionalized with a nonspecific antibody and shows no binding. (D) Reference-compensated detection response to mouse IgG in human serum (10%) in PBS, on a polymer brush surface functionalized with an antibody against mouse IgG.

of bioreceptor would be to tune the relative thicknesses of the polymer blocks to obtain a higher ratio of the blocks of poly(HOEGMA) to poly(MeOEGMA). However, in our previous work concerning the functionalization of hierarchically structured antifouling polymer brushes, a trade-off between the immobilized amount of bioreceptors and the antifouling performance was observed.[16]

The fouling from undiluted blood plasma and serum, two of the most challenging biological matrices encountered in biosensing, was also quantified by SPR and was found to be (35.8 ± 1.3) ng·cm^{-2} and (35.5 ± 3.6) ng·cm^{-2}, respectively (example sensograms are shown in Figure S3 in the Supporting Information). This represents a reduction of close to 90% in comparison to bare gold and is on a comparable level with other available state-of-the-art functionalized antifouling surfaces.[16,44,45]

In Situ Fabrication of a Model Biosensing Platform. In order to illustrate an example application of our precision biofunctionalization for the fabrication of a truly functional and bioactive surface, the capability of the streptavidin-functional polymer brushes to immobilize model biotin-conjugated antibodies was examined by SPR. Antibodies are commonly employed as biorecognition elements in the fabrication of biosensors as well as for the capture of other target molecules or cells. Furthermore, biotin conjugates of antibodies are widely available commercially as they are often used in immunoassays and the technology for their production is well developed. The rapid immobilization of a biotinylated rabbit antibody and a biotinylated polyclonal goat antibody against mouse IgG was observed when the surface was contacted with 50 μg·mL^{-1} antibody solutions in PBS for 10 min in two independent flow cell channels in the SPR setup (Figure 3B), reaching immobilization densities of 17 and 21 ng·cm^{-2}, respectively. To evidence the activity and specificity of the antibody-functionalized surfaces, a solution of mouse IgG (50 μg·mL^{-1} in PBS) was subsequently injected on both channels for 10 min. The sensogram obtained shows how the specific antibody against the model analyte is able to capture and immobilize it from the solution, while the surface presenting a nonspecific antibody shows no interaction. Thus, the specificity of the capture is confirmed, while the nonspecific adsorption or capture of the mouse IgG can be excluded. The ability to achieve the spatially resolved immobilization of biorecognition elements on antifouling polymer brushes, accessible through the phototriggered ligation employed, is of particular interest for biosensing applications such as SPR imaging and protein arrays.[46−48] Furthermore, the ability to capture mouse IgG from diluted human serum (10% in PBS) was examined by spiking the solution with the model analyte. Figure 3D shows the reference-compensated response as the difference between the signals in the detection channel and a reference channel (nonspiked 10% human serum) measured simultaneously. The analyte is rapidly detected in diluted serum giving a signal of similar magnitude as in PBS, confirming the potential of the surface for biosensing applications.

Spatially Resolved Grafting of Poly(carboxybetaine acrylamide). Given the importance of the precise control not only of the chemistry, but also of the macromolecular architecture of antifouling polymer brushes, we exploited this functionalization strategy to design a more complex structure. The polymer brushes presenting tetrazole-functional side chains were employed to create a hierarchical macromolecular architecture of the type graft-on-graft. A maleimide incorporating a tertiary alkyl bromide group (1 mg·mL^{-1} in DCM)[5] was immobilized by the attachment to the tetrazole-moieties in the top block of the polymer brushes under UV light irradiation. Thus, the side chains of this polymer region were effectively rendered into initiators for a successive step of SI-ATRP.

Before the photoligation of the maleimide-ATRP-initiator, the Br chain ends were replaced with azide via a nucleophilic substitution with NaN_3 (3.4 mg·mL^{-1} in DMF at 50 °C for 3 h).[49] Thus, we prevent further chain extension from the polymer end groups during the graft-on-graft polymerization, thereby confining the growth to irradiated areas. The third polymer block consisted of poly(carboxybetaine acrylamide)

DOI: 10.1021/acs.langmuir.5b01114
Langmuir XXXX, XXX, XXX−XXX

(poly(CBAA)), a zwitterionic polymer which has been shown to have ultralow fouling properties.[33] The total layer thickness for the triblock structure reached 42 nm, yielding a thickness increment of 7 nm after the poly(CBAA) block. XPS further confirmed the success of the grafting of poly(CBAA) by evidencing the presence of the expected features for the polymer, namely, two signals in the N 1s region corresponding to the amide (399.8 eV) and the quaternary ammonium (402.5 eV) (Figure 4B).[28] Moreover, the C 1s region's spectrum reveals a relative increase in the content of carbon stemming from C−C or C−H bonds.

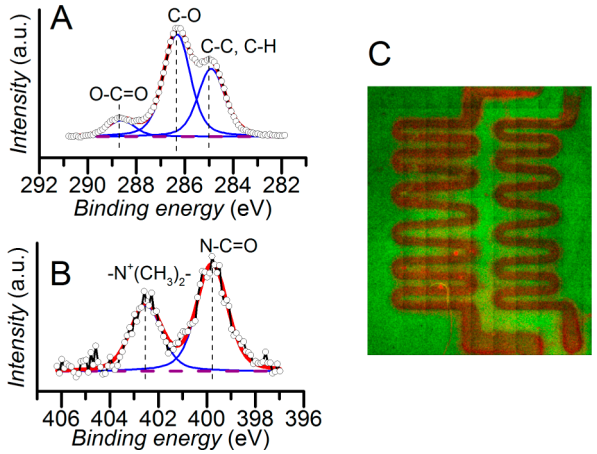

Figure 4. Grafting of poly(CBAA). High-resolution XPS spectra of the C 1s (A) and N 1s (B) regions. (C) ToF-SIMS image showing an overlay of CN^- (red, arising from the poly(CBAA) block) and the ethylene glycol fragments $C_2H_3O^-$ and $C_4H_5O_2^-$ (green).

In order to unambiguously evidence that the poly(CBAA) block was grown from the initiator moiety clicked onto the tetrazole, the same procedure was applied using a shadow mask to restrict the irradiation with UV light to the wave-shaped opening and the resulting surfaces were analyzed by ToF-SIMS (Figure 4C). An increase in the counts for CN^- as well as a decrease for the fragments arising for the ethylene glycol side chains of the underlying polymer blocks are observed for the patterned area, confirming the localization of the newly grown poly(CBAA).

CONCLUSIONS

In summary, we have demonstrated the introduction of photoactive tetrazole units to hierarchically structured polymer brushes. These were employed for the localized immobilization of streptavidin through the phototriggered ligation of a maleimide-containing biotin. An example application of the streptavidin-functionalized polymer brushes was demonstrated with a model biosensor showing the specific capture of a model analyte in PBS and serum by an immobilized antibody. Furthermore, an ATRP initiator was also selectively attached to the side chains of the top block of the polymer brush. This enabled the growth of a further polymer block in a graft-on-graft architecture. The strategy introduced through these two examples permits functionalization of antifouling polymer brushes under mild conditions via the immobilization of maleimide-containing molecules, while simultaneously adding the possibility of patterning via a UV lithographic process. Thus, a substantial increase in the accessible complexity for the bottom-up design of surface architectures has been achieved, adding a valuable tool to attain precisely engineered bioactive surfaces.

ASSOCIATED CONTENT

Supporting Information

Chemical characterization of the polymer brushes after the phototriggered functionalization reactions, confirmation of the specificity of the immobilization of streptavidin, imaging the conversion of the tetrazole groups by ToF-SIMS, and example SPR sensograms of the measurement of fouling from blood plasma and serum. The Supporting Information is available free of charge on the ACS Publications website at DOI: 10.1021/acs.langmuir.5b01114.

AUTHOR INFORMATION

Corresponding Authors

*E-mail: rodriguez@imc.cas.cz; Fax: +420 296 809 410; Tel: +420 296 809 333 (C.R.-E.).

*E-mail: christopher.barner-kowollik@kit.edu. Web: http://www.macroarc.de (C.B.-K.).

Notes

The authors declare no competing financial interest.

ACKNOWLEDGMENTS

The work was supported by the Program of Project Based Personal Exchange ASCR-DAAD (no. 14/08), the Grant Agency of the Czech Republic (GACR) under contract no. 15-09368Y, and the European Regional Development Funds under the project "BIOCEV − Biotechnology and Biomedicine Centre of the Academy of Sciences and Charles University" (CZ.1.05/1.1.00/02.0109) and OPPK CZ.2.16/3.1.00/21545. C.B.-K. thanks the German Academic Exchange Service (DAAD) for funding a research stay of A.S.P. and N.K. at the Karlsruhe Institute of Technology (KIT). C.B.-K. additionally acknowledges support for the project from the BioInterfaces program of the Helmholtz association at the KIT.

REFERENCES

(1) Blaszykowski, C.; Sheikh, S.; Thompson, M. Surface chemistry to minimize fouling from blood-based fluids. *Chem. Soc. Rev.* **2012**, *41* (17), 5599−5612.

(2) Blaszykowski, C.; Sheikh, S.; Thompson, M. Biocompatibility and antifouling: Is there really a link? *Trends Biotechnol.* **2014**, *32* (2), 61−62.

(3) Yu, Q.; Zhang, Y.; Wang, H.; Brash, J.; Chen, H. Anti-fouling bioactive surfaces. *Acta Biomater.* **2011**, *7* (4), 1550−1557.

(4) Xu, F. J.; Neoh, K. G.; Kang, E. T. Bioactive surfaces and biomaterials via atom transfer radical polymerization. *Prog. Polym. Sci.* **2009**, *34* (8), 719−761.

(5) Rodriguez-Emmenegger, C.; Preuss, C. M.; Yameen, B.; Pop-Georgievski, O.; Bachmann, M.; Mueller, J. O.; Bruns, M.; Goldmann, A. S.; Bastmeyer, M.; Barner-Kowollik, C. Controlled cell adhesion on poly(dopamine) interfaces photopatterned with non-fouling brushes. *Adv. Mater.* **2013**, *25* (42), 6123−6127.

(6) Ma, H.; Hyun, J.; Stiller, P.; Chilkoti, A. "Non-fouling" oligo(ethylene glycol)—Functionalized polymer brushes synthesized by surface-initiated atom transfer radical polymerization. *Adv. Mater.* **2004**, *16* (4), 338−341.

(7) Hucknall, A.; Kim, D. H.; Rangarajan, S.; Hill, R. T.; Reichert, W. M.; Chilkoti, A. Simple Fabrication of Antibody Microarrays on Nonfouling Polymer Brushes with Femtomolar Sensitivity for Protein Analytes in Serum and Blood. *Adv. Mater.* **2009**, *21* (19), 1968−1971.

(8) Gautrot, J. E.; Huck, W. T.; Welch, M.; Ramstedt, M. Protein-resistant NTA-functionalized polymer brushes for selective and stable

DOI: 10.1021/acs.langmuir.5b01114
Langmuir XXXX, XXX, XXX−XXX

immobilization of histidine-tagged proteins. *ACS Appl. Mater. Interfaces* **2010**, *2* (1), 193−202.
(9) Barbey, R.; Lavanant, L.; Paripovic, D.; Schuwer, N.; Sugnaux, C.; Tugulu, S.; Klok, H. A. Polymer brushes via surface-initiated controlled radical polymerization: Synthesis, characterization, properties, and applications. *Chem. Rev.* **2009**, *109* (11), 5437−527.
(10) Krishnamoorthy, M.; Hakobyan, S.; Ramstedt, M.; Gautrot, J. E. Surface-initiated polymer brushes in the biomedical field: Applications in membrane science, biosensing, cell culture, regenerative medicine and antibacterial coatings. *Chem. Rev.* **2014**, *114* (21), 10976−1026.
(11) Gunkel, G.; Weinhart, M.; Becherer, T.; Haag, R.; Huck, W. T. Effect of polymer brush architecture on antibiofouling properties. *Biomacromolecules* **2011**, *12* (11), 4169−4172.
(12) Huang, C. J.; Li, Y.; Jiang, S. Zwitterionic polymer-based platform with two-layer architecture for ultra low fouling and high protein loading. *Anal. Chem.* **2012**, *84* (7), 3440−3445.
(13) Peng, S. J.; Bhushan, B. Smart polymer brushes and their emerging applications. *RSC Adv.* **2012**, *2* (23), 8557−8578.
(14) Chen, Y. X.; Triola, G.; Waldmann, H. Bioorthogonal chemistry for site-specific labeling and surface immobilization of proteins. *Acc. Chem. Res.* **2011**, *44* (9), 762−73.
(15) Tugulu, S.; Arnold, A.; Sielaff, I.; Johnsson, K.; Klok, H. A. Protein-functionalized polymer brushes. *Biomacromolecules* **2005**, *6* (3), 1602−1607.
(16) de los Santos Pereira, A.; Riedel, T.; Brynda, E.; Rodriguez-Emmenegger, C. Hierarchical antifouling brushes for biosensing applications. *Sens. Actuators, B* **2014**, *202*, 1313−1321.
(17) Trmcic-Cvitas, J.; Hasan, E.; Ramstedt, M.; Li, X.; Cooper, M. A.; Abell, C.; Huck, W. T.; Gautrot, J. E. Biofunctionalized protein resistant oligo(ethylene glycol)-derived polymer brushes as selective immobilization and sensing platforms. *Biomacromolecules* **2009**, *10* (10), 2885−2894.
(18) Orski, S.; Sheppard, G.; Arnold, R.; Grubbs, J.; Locklin, J. Post-polymerization modification of polymer brushes. In *Functional Polymers by Post-Polymerization Modification: Concepts, Guidelines, and Applications*; Theato, P., Klok, H. A., Eds.; Wiley-VCH Verlag GmbH & Co. KGaA: Weinheim, Germany, 2012.
(19) Sheikh, S.; Sheng, J. C. C.; Blaszykowski, C.; Thompson, M. New oligoethylene glycol linkers for the surface modification of an ultra-high frequency acoustic wave biosensor. *Chem. Sci.* **2010**, *1* (2), 271−275.
(20) Ayres, N. Polymer brushes: Applications in biomaterials and nanotechnology. *Polym. Chem.* **2010**, *1* (6), 769−777.
(21) Ebara, M.; Yamato, M.; Aoyagi, T.; Kikuchi, A.; Sakai, K.; Okano, T. A novel approach to observing synergy effects of PHSRN on integrin−RGD binding using intelligent surfaces. *Adv. Mater.* **2008**, *20* (16), 3034−3038.
(22) Kuzmyn, A. R.; de los Santos Pereira, A.; Pop-Georgievski, O.; Bruns, M.; Brynda, E.; Rodriguez-Emmenegger, C. Exploiting end group functionalization for the design of antifouling bioactive brushes. *Polym. Chem.* **2014**, *5* (13), 4124−4131.
(23) Tischer, T.; Claus, T. K.; Bruns, M.; Trouillet, V.; Linkert, K.; Rodriguez-Emmenegger, C.; Goldmann, A. S.; Perrier, S.; Börner, H. G.; Barner-Kowollik, C. Spatially controlled photochemical peptide and polymer conjugation on biosurfaces. *Biomacromolecules* **2013**, *14* (12), 4340−4350.
(24) Jonkheijm, P.; Weinrich, D.; Kohn, M.; Engelkamp, H.; Christianen, P. C.; Kuhlmann, J.; Maan, J. C.; Nusse, D.; Schroeder, H.; Wacker, R.; Breinbauer, R.; Niemeyer, C. M.; Waldmann, H. Photochemical surface patterning by the thiol-ene reaction. *Angew. Chem., Int. Ed. Engl.* **2008**, *47* (23), 4421−4424.
(25) Lin, P. C.; Weinrich, D.; Waldmann, H. Protein Biochips: Oriented Surface Immobilization of Proteins. *Macromol. Chem. Phys.* **2010**, *211* (2), 136−144.
(26) Orski, S. V.; Poloukhtine, A. A.; Arumugam, S.; Mao, L.; Popik, V. V.; Locklin, J. High density orthogonal surface immobilization via photoactivated copper-free click chemistry. *J. Am. Chem. Soc.* **2010**, *132* (32), 11024−11026.
(27) Preuss, C. M.; Tischer, T.; Rodriguez-Emmenegger, C.; Zieger, M. M.; Bruns, M.; Goldmann, A. S.; Barner-Kowollik, C. A bioinspired light induced avenue for the design of patterned functional interfaces. *J. Mater. Chem. B* **2014**, *2* (1), 36−40.
(28) Tischer, T.; Rodriguez-Emmenegger, C.; Trouillet, V.; Welle, A.; Schueler, V.; Mueller, J. O.; Goldmann, A. S.; Brynda, E.; Barner-Kowollik, C. Photo-patterning of non-fouling polymers and biomolecules on paper. *Adv. Mater.* **2014**, *26* (24), 4087−4092.
(29) Glassner, M.; Oehlenschlaeger, K. K.; Welle, A.; Bruns, M.; Barner-Kowollik, C. Polymer surface patterning via Diels−Alder trapping of photo-generated thioaldehydes. *Chem. Commun. (Cambridge, U. K.)* **2013**, *49* (6), 633−5.
(30) Wang, Y.; Hu, W. J.; Song, W.; Lim, R. K.; Lin, Q. Discovery of long-wavelength photoactivatable diaryltetrazoles for bioorthogonal 1,3-dipolar cycloaddition reactions. *Org. Lett.* **2008**, *10* (17), 3725−3728.
(31) Yu, Z.; Ho, L. Y.; Wang, Z.; Lin, Q. Discovery of new photoactivatable diaryltetrazoles for photoclick chemistry via 'scaffold hopping'. *Bioorg. Med. Chem. Lett.* **2011**, *21* (17), 5033−5036.
(32) Jones, D. M.; Brown, A. A.; Huck, W. T. S. Surface-initiated polymerizations in aqueous media: Effect of initiator density. *Langmuir* **2002**, *18* (4), 1265−1269.
(33) Rodriguez-Emmenegger, C.; Hasan, E.; Pop-Georgievski, O.; Houska, M.; Brynda, E.; Alles, A. B. Controlled/living surface-initiated ATRP of antifouling polymer brushes from gold in PBS and blood sera as a model study for polymer modifications in complex biological media. *Macromol. Biosci.* **2012**, *12* (4), 525−532.
(34) Rodriguez-Emmenegger, C.; Kylian, O.; Houska, M.; Brynda, E.; Artemenko, A.; Kousal, J.; Alles, A. B.; Biederman, H. Substrate-independent approach for the generation of functional protein resistant surfaces. *Biomacromolecules* **2011**, *12* (4), 1058−1066.
(35) Parry, K. L.; Shard, A. G.; Short, R. D.; White, R. G.; Whittle, J. D.; Wright, A. ARXPS characterisation of plasma polymerised surface chemical gradients. *Surf. Interface Anal.* **2006**, *38* (11), 1497−1504.
(36) Scofield, J. H. Hartree−Slater subshell photoionization cross-sections at 1254 and 1487 eV. *J. Electron Spectrosc. Relat. Phenom.* **1976**, *8* (2), 129−137.
(37) Tanuma, S.; Powell, C. J.; Penn, D. R. Calculations of electron inelastic mean free paths. V. Data for 14 organic compounds over the 50−2000 eV range. *Surf. Interface Anal.* **1994**, *21* (3), 165−176.
(38) Homola, J. Surface plasmon resonance sensors for detection of chemical and biological species. *Chem. Rev.* **2008**, *108* (2), 462−93.
(39) Ma, H.; Li, D.; Sheng, X.; Zhao, B.; Chilkoti, A. Protein-resistant polymer coatings on silicon oxide by surface-initiated atom transfer radical polymerization. *Langmuir* **2006**, *22* (8), 3751−3756.
(40) Pop-Georgievski, O.; Rodriguez-Emmenegger, C.; de los Santos Pereira, A.; Proks, V.; Brynda, E.; Rypáček, F. Biomimetic non-fouling surfaces: Extending the concepts. *J. Mater. Chem. B* **2013**, *1*, 2859−2867.
(41) Fan, X.; Lin, L.; Dalsin, J. L.; Messersmith, P. B. Biomimetic anchor for surface-initiated polymerization from metal substrates. *J. Am. Chem. Soc.* **2005**, *127* (45), 15843−15847.
(42) Riedel, T.; Rodriguez-Emmenegger, C.; de los Santos Pereira, A.; Bedajankova, A.; Jinoch, P.; Boltovets, P. M.; Brynda, E. Diagnosis of Epstein−Barr virus infection in clinical serum samples by an SPR biosensor assay. *Biosens. Bioelectron.* **2014**, *55*, 278−84.
(43) Love, J. C.; Estroff, L. A.; Kriebel, J. K.; Nuzzo, R. G.; Whitesides, G. M. Self-assembled monolayers of thiolates on metals as a form of nanotechnology. *Chem. Rev.* **2005**, *105* (4), 1103−1169.
(44) Vaisocherova, H.; Zhang, Z.; Yang, W.; Cao, Z.; Cheng, G.; Taylor, A. D.; Piliarik, M.; Homola, J.; Jiang, S. Functionalizable surface platform with reduced nonspecific protein adsorption from full blood plasma—Material selection and protein immobilization optimization. *Biosens. Bioelectron.* **2009**, *24* (7), 1924−1930.
(45) Vaisocherova, H.; Sevcu, V.; Adam, P.; Spackova, B.; Hegnerova, K.; de los Santos Pereira, A.; Rodriguez-Emmenegger, C.; Riedel, T.; Houska, M.; Brynda, E.; Homola, J. Functionalized ultra-low fouling carboxy- and hydroxy-functional surface platforms: Functionalization

DOI: 10.1021/acs.langmuir.5b01114
Langmuir XXXX, XXX, XXX−XXX

capacity, biorecognition capability and resistance to fouling from undiluted biological media. *Biosens. Bioelectron.* **2014**, *51*, 150−157.
(46) Scarano, S.; Mascini, M.; Turner, A. P.; Minunni, M. Surface plasmon resonance imaging for affinity-based biosensors. *Biosens. Bioelectron.* **2010**, *25* (5), 957−966.
(47) Shumaker-Parry, J. S.; Zareie, M. H.; Aebersold, R.; Campbell, C. T. Microspotting streptavidin and double-stranded DNA arrays on gold for high-throughput studies of protein−DNA interactions by surface plasmon resonance microscopy. *Anal. Chem.* **2004**, *76* (4), 918−929.
(48) Rusmini, F.; Zhong, Z.; Feijen, J. Protein immobilization strategies for protein biochips. *Biomacromolecules* **2007**, *8* (6), 1775−1789.
(49) Brault, N. D.; Sundaram, H. S.; Huang, C. J.; Li, Y.; Yu, Q.; Jiang, S. Two-layer architecture using atom transfer radical polymerization for enhanced sensing and detection in complex media. *Biomacromolecules* **2012**, *13* (12), 4049−56.

DOI: 10.1021/acs.langmuir.5b01114
Langmuir XXXX, XXX, XXX−XXX